Airborne Gravity Data Adjustment Using a Cross-Over Adjustment with Constraints

Srimanee, C.,[1] Dumrongchai, P.,[1,*] and Duangdee, N.[2]
[1]Department of Civil Engineering, Faculty of Engineering, Chiang Mai University, Chiang Mai, Thailand
E-mail: chawis.s@cmu.ac.th, puttipol.d@cmu.ac.th
[2]Royal Thai Survey Department, Royal Thai Armed Forces Headquarters, Thailand
**Corresponding author*

Abstract

The Royal Thai Survey Department (RTSD), in cooperation with Chiang Mai University, directed airborne gravimetry across Thailand from 2016 to 2017. This made it possible to conduct surveys in inaccessible locations such as mountainous and coastal areas. The gravimeter that was integrated with GPS/GNSS receiver on board together with one gravity base station on the ground measured airborne free-air anomalies (FAA) at an average of 4,000m flight height above MSL with a speed of 200 knots and a 20 Hz measuring rate. The main flight lines were in a north-south direction, while east-west direction lines were supplementary and used to determine the observation quality of the measured FAA. Theoretically, the intersections between the main and supplementary flight lines should have been equal. However, gravity data is greatly affected by air turbulence from weather variations, causing large differences in values at those points. The study area included three operating blocks of geoid development projects conducted in the Chao Phraya River basin. These projects covered the northern and central regions of the country. This study focuses on improving airborne gravity through cross-over adjustments using a least-square adjustment with constraints. The observations were first inspected and edited, and then the FAA differences (FAAD) of 477 intersections were adjusted. The results from the adjustment of three blocks show that the root mean square (RMS) decreased from 3.9 to 2.6 milligals (mGals). Geoid models from both adjusted and non-adjusted airborne gravity data were determined. The geoidal heights of both models were compared with the geoidal height of 184 GNSS/Leveling co-points. The comparative results showed an improvement in accuracy of the adjusted airborne geoid model at a centimetre level.

1. Introduction

The development of airborne geoid determination increased as a result of the development of GPS in the early 1980s, allowing for improved measurement efficiency (Li, 2000). Techniques and tools have been developed to provide more accurate gravitational data, particularly in the commercial sectors (Forsberg et al., 2015). In addition, research conducted by Li (2000), Olesen (2003), Forsberg et al., (2000) and Hwang et al., (2007) have shown better results, with airborne gravitational measurements achieving accuracies of 2-4 mGal RMS. It is now more acceptable to use airborne gravity data in conjunction with terrestrial gravity data for precise geoid model determinations. In a collaboration between the Royal Thai Survey Department and Chiang Mai University from 2015 – 2017, Thailand developed a precise geoid model, TGM2017 (Dumrongchai and Duangdee, in press), to replace the local geoid of Thailand, THAI12H (Dumrongchai et al., 2012). In general, terrestrial gravimetry (TTG) can only be done in accessible areas with a determined spatial resolution. This is different from airborne gravimetry (ABG) that can cover a whole area but has inferior spatial resolution. Therefore, this project gathered terrestrial and airborne gravity measurements to obtain gravity data covering the whole country. ABG is an effective gravity measurement technique, and many studies of geoid determination have used airborne gravity data, such as Bayoud and Sideris (2002), Albert and Klees (2004), Forsberg (2005), Hwang et al., (2007) and Dumrongchai et al., (2017).

The airborne gravity data in this research was obtained using a TAGS6 Micro-g gravimeter (Micro-g LaCoste, 2015b) integrated with a GPS/GNSS receiver installed in a Beechcraft Super King Air model B200. The gravimeter recorded airborne free-air gravity anomaly (FAA) data. It had a 20 Hz measuring rate, 200-knot speed, had a flight altitude of about 4,000m above mean sea level and its gravitational potential measure unit was in mGal. The study area included three of the seven blocks (Blocks 1-3) of a project conducted in the Chao Phraya River basin, located in the northern and central regions of the country. In each designated research block area, the main flight line, along-track, operated in a north-south direction with 10km spacing. The supplementary flight lines, cross-tracks, were flown in an east-west direction with a 50km spacing to determine observation quality (Figure 1.) At the track cross-over points, the FAA measures of the lines should theoretically be equal. However, flight operations data showed various magnitudes of observation deviations, which were affected by air turbulence from the monsoon season.

This article focuses on how to improve airborne gravity data to support precise geoid model determinations. Cross-over adjustments were used to modify the linear characteristics of each survey line. The goal was to reduce FAA differences at the cross points of along-tracks and cross-tracks using a least-square adjustment with a constraints technique (Koch, 1999, Forsberg et al., 2000, Surpas, 2003, Forsberg, 2005, and Srimanee, 2018). In addition, we considered the number and location of the constraints, air-control, and points of the three overlap blocks adjustment. The unadjusted FAA was inspected and edited only and the adjusted FAA was edited and had a cross-over adjustment. These were the inputs used for airborne geoid determinations and used a least-squares collocation (LSC) for downward continuation (DWC) of airborne form flying height to the surface. The geoid models were then analysed using Molodensky's approach. The resulting geoid models verified accuracy by comparing geoidal heights with the national control datum at GNSS/Leveling co-point locations within the study area.

2. Airborne Gravimetry

The basic principle of airborne gravimetry is based on Newton's second law of motion under the influence of Earth's gravity field (Li, 2000), expressed by three vector components as:

$$\ddot{X} = a + \bar{g}$$

Equation 1

where $\ddot{X}$ is the total or kinematic acceleration, m/s^2, of the moving object that is the sum of a, the special force or acceleration of an airplane, and $\bar{g}$, the gravitational force that influences an airplane without centrifugal force. Airplane positions were measured using an on-board GPS that synced with the gravimeter and referred to at least one base station on the ground (Albert and Klees, 2004.)

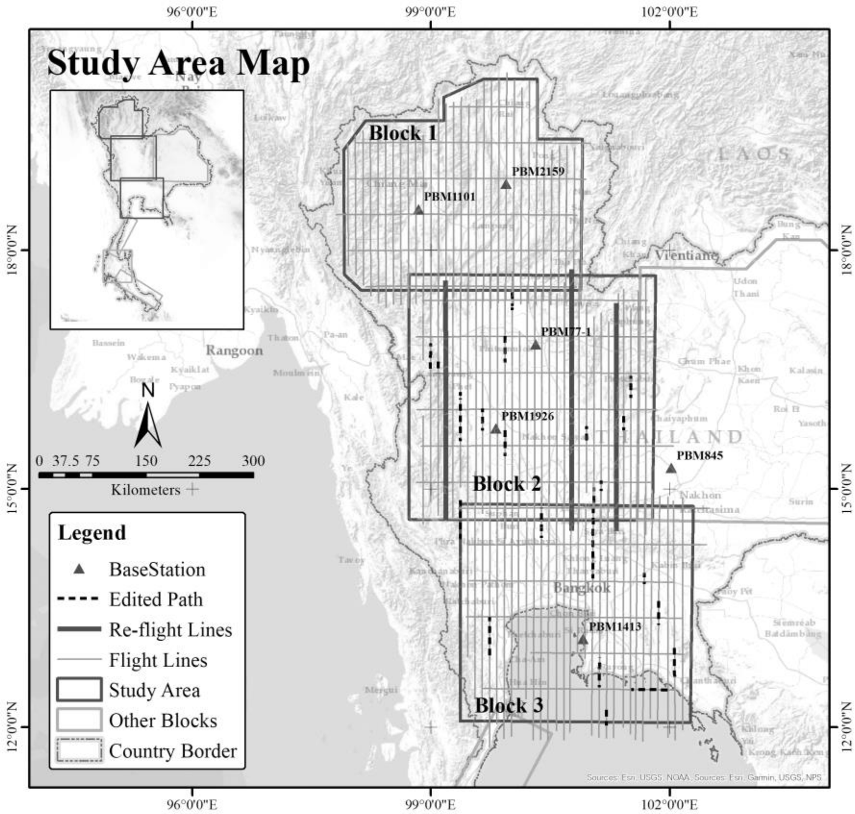

Figure 1: The study area and the flight lines of airborne gravimetry including the editing paths and re-flight operations in lines 106, 123 and 129 of Blocks 1 and 2

The vector a was provided by a gravimeter at each point. Thus, the $\bar{g}$ of each point was computed from both vectors $\ddot{X}$ And a. At the flight height, the basic concept of free-air gravity anomaly is as follows (Forsberg et al., 2000):

$$\Delta g = g - \frac{\partial^2 h_{GPS}}{\partial t^2} + C_{eot} - \gamma_0 + \frac{\partial \gamma}{\partial h}(h_{GPS} - N_{EGM})$$

Equation 2

where g is the measured gravimetry (mGal), h_{GPS} is the ellipsoidal height, C_{eot} is the Eötvös correction, γ_0 is the normal (ellipsoidal) gravity, and the geoid height N is from EGM2008 (Pavlis et al., 2012). As a relative type gravimeter was used in the geoid model project, the airplane had to park at the hanger's gravity base station for base readings before and after the flight operation in order to link the airborne gravity data to the ground station. The FAA equation is expressed as:

$$\Delta g = f_Z - \ddot{h} + \delta g_{eot} + \delta g_{tilt} - f_0 + g_0 - (\gamma_0 + \frac{\partial \gamma}{\partial h}(h_{GPS} - N_{EGM08}) + \frac{1 \partial^2 \gamma}{2 \partial h^2}(h_{GPS} - N_{EGM08})^2)$$

Equation 3

where f_0 is the base reading gravity data (mGal), g_0 is the gravity data of base station, f_Z is gravity data at the flight altitude, $\ddot{h}$ is the vertical acceleration received from the onboard GPS, δg_{eot} is the Eötvös correction, δg_{tilt} is the off-vertical or tilt correction, γ_0 is the normal gravity, and N_{EGM08} is the EGM2008 geoid undulation (see Moritz, 1980 for more details.). The airborne gravimetry in Thailand was firstly planned to cover the entire country. However, due to both the performance of aircraft equipped with gravimeter sets and the physical characteristics of Thailand, the survey area was designed limited to seven blocks in order to obtain gravity data covering all regions of the country.

We selected a study area within the Chao Phraya basin. Figure 1 shows the airborne surveys conducted in Blocks 1, 2 and 3. These areas covered much of the northern through central parts of the country. The physical characteristics of the study area included mountains in the north and flat areas in the central region.

The TAGS-6 Micro-g gravimeter installed in the Beechcraft Super King Air model B200 aircraft was integrated with a Novatel DL-V3 GPS/GNSS. Table 1 describes the characteristics of airborne gravity surveying. The survey flight lines crossed over the block areas in two directions. The main flight lines, along-track, were in a north-south direction and had 10km spacing. The supplementary lines, cross-track, were in an east-west direction with 50km spacing and served as checking lines to monitor the quality of the main lines. The RTSD selected the Phitsanulok airport as the aircraft landing base for Block 1, and chose six GPS/GNSS based-stations within the appropriate range of 150km. These stations were in national networks that referred to the international reference ITRF2008 at epoch 2013.10, and Kolak datum for heights above mean sea level (MSL).

The accuracy of kinematic positioning was about 5cm, sufficient for geoid determination by airborne gravimetry. There were a total of 95 along-track lines and 20 supplementary cross-tracks. he airborne gravimetry of the study area was conducted from May to December 2016. T Blocks 1 and 2 were measured during the monsoon season. Although the TAGS-6 had a versatile stabilization system, some flight lines were significantly affected by severe air turbulence, deteriorating the quality of the observation data. Figure 1 shows that over half of the flight lines 106, 123 and 129 in Block 1 contained unusable FAA. Re-flight operations were necessary. The airborne raw data in both along and cross-tracks were manipulated to improve their gravity data quality. The work procedure used in this study is shown in Figure 2.

Table 1: Airborne gravimetry details of Blocks 1, 2 and 3

Flight characteristics	**Description**		
	Block 1	**Block 2**	**Block 3**
Flight altitude (MSL)	3000 - 4000m	4000m	4000m
Ground speed (knots/km per hour)	200/370	200/370	200/370
Data sampling	1Hz or 5km.	1Hz or 5km.	1Hz or 5km.
Along & cross-track spacing (km)	10 & 50	10 & 50	10 & 50
No. of along & cross-tracks	31 & 7 lines	31 & 6 lines	33 & 6 lines
Along/cross-track distances (km)	~338/ ~330	~300/ ~320	~300/ ~320
No. of cross-over points	177	139	161
GPS/GNSS Base stations	3	3	2

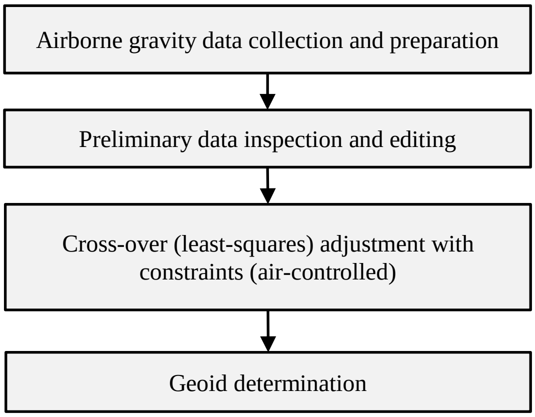

Figure 2: The study workflow

3. Airborne Gravimetry Data Processing

The raw gravity data was filtered using a 90-second Butterworth filter (Micro-g, LaCost, 2015a), and the filtered gravity data was compared to data from an Earth Gravitational Model 2008 (EGM2008) that was acquired at the same location and altitude. The findings should not have differed more than ±20mGals from the average of EGM2008, the limits of acceptable gravity data quality under most circumstances in Thailand (adapted from Damiani and Youngman, 2015.) However, as shown in the dash-rectangle (Figure 3a), there were huge differences at both ends of each survey line, and these paths were trimmed out. If such errors occurred within a flight line, as shown in the dash-circle of line 108 of Block 1, other related measurement information obtained at the same time and location - including beam movement and the number of high vertical accelerations - were considered in our decision to either remove data or re-flight (Figure 3b). The excess values of differences should not have contained more than 20 percent of one data line. The beam position in TAGS-6 should have been in the interval of ±0.005 units, and the count number of the aircraft vertical acceleration should not have exceeded the limits of ±50,000 TAGS-6-units (Figure 3c). Contaminated gravity values were removed if the differences exceeded these limits. The re-calculated values, based on EGM2008, were adjusted to fill in those lines using a simple least-squares adjustment. However, as illustrated in Figure 1, if either the beam or the speed change was out of bounds for more than 50% of the entire flight, then a re-flight was required. Three lines of Block 1 had to re-flight, including106, 123 and 129.

4. Cross-Over Adjustment with Constraints

A least-square adjustment (LSA) with constraints served as a tool for cross-over adjustment to improve airborne gravity data self-consistency. The linear characteristics of each survey line that were included in the filtered gravity data provided by AGSys6 processing software (Micro-g LaCoste, 2015b) had to be adjusted to eliminate the FAAD at intersections between the along-track and the cross-tracks to ensure consistency of the whole observation. For constraint conditions, the cross-over points or so-called air-controlled points were optimally selected based on the assumption that observations at intersections between along-tracks and cross-tracks should be equal. An LSA with a constraint condition technique (Hwang et al., 2007 and Koch, 1999) was used to minimize the discrepancies at the crossing points. The geometry of the flight lines and cross-over points are shown in Figure 4. The LSA was based on an observation equations method. At intersections, the measured FAA of along-track and cross-track are denoted by $y_{ai(pi,qi)}$ and $y_{ci(pi,qi)}$ respectively with i = 1-n. The bias and trend parameters of line ai, and ci are denoted by b_{ai}, m_{ai}, and b_{ci}, m_{ci} respectively. The adjusted FAA on both lines are denoted by $Y_{ai(pi,qi)}$, $Y_{ci(pi,qi)}$. Then for the line $c1$, a set of equations is written as follows:

$$y_{ai(pi,q1)} = Y_{ai(pi,q1)} + b_{ai} + m_{ai}(q1 - q0) + e_{ai(pi,q1)}$$
Equation 4

$$y_{c1(p1,qi)} = Y_{c1(p1,qi)} + b_{c1} + m_{c1}(pi - p0) + e_{c1(p1,qi)}$$
Equation 5

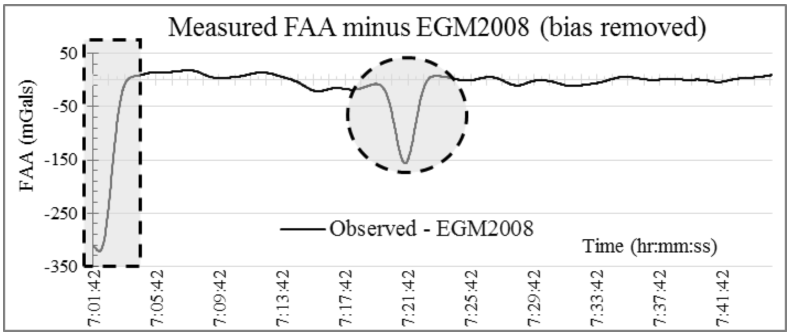

Figure 3a: The bias removal difference between the measured FAA and EGM2008

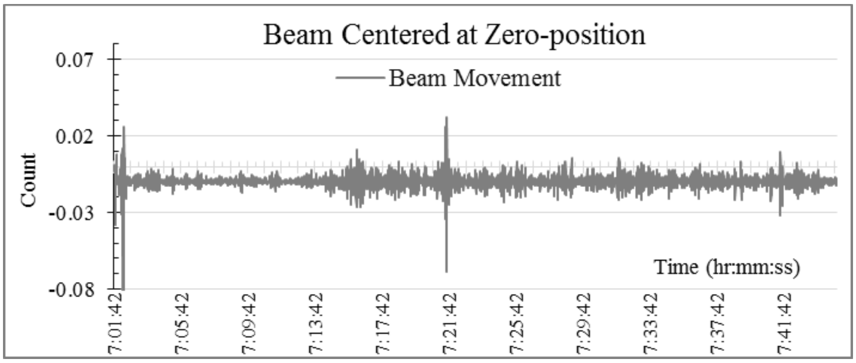

Figure 3b: A graph of beam movement during flight measurement

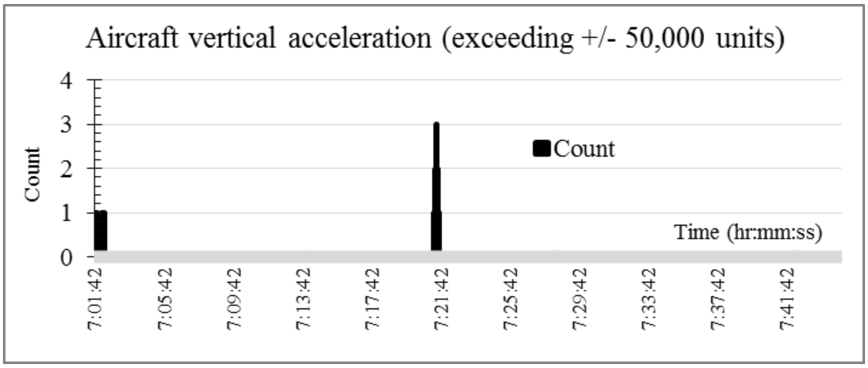

Figure 3c: Count number of the aircraft vertical acceleration exceeding +/- 50,000 TAGS-6 units

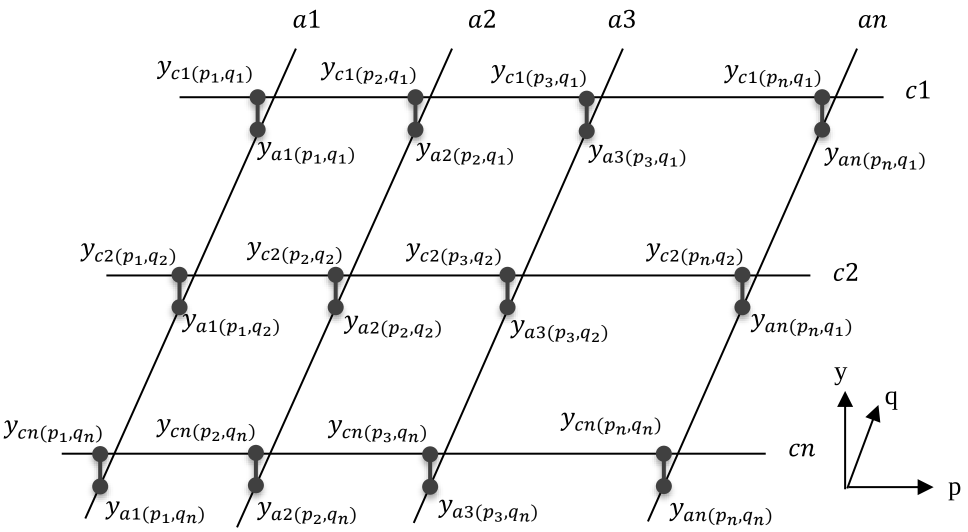

Figure 4: Schematic representation of along tracks, cross tracks, and cross-over points

Where pi refers to the latitude position, qi refers to the longitude position of each intersection, and $p0$ and $q0$ represent the coordinates of the given origin of the three blocks. For the C_2 line, we have:

$$y_{ai(pi,q2)} = Y_{ai(pi,q2)} + b_{ai} + m_{ai}(q2 - q0) + e_{a1(pi,q2)} \quad \text{Equation 6}$$

$$y_{c2(pi,q2)} = Y_{c2(pi,q2)} + b_{c2} + m_{c2}(pi - p0) + e_{c2(pi,q2)} \quad \text{Equation 7}$$

The difference of each intersection was formed by subtractions of along-tracks and cross-tracks. We have:

$$
\begin{aligned}
y_{a1(p1,q1)} - y_{c1(p1,q1)} &= b_{a1} + m_{a1}(q1 - q0) - b_{c1} - m_{c1}(p1 - p0) + e_{a1(p1,q1),c1(p1,q1)} \\
y_{a2(p2,q1)} - y_{c1(p2,q1)} &= b_{a2} + m_{a2}(q2 - q0) - b_{c1} + m_{c1}(p2 - p0) + e_{a2(p2,q1),c1(p2,q1)} \\
y_{an(pn,q1)} - y_{c1(pn,q1)} &= b_{an} + m_{an}(qn - q0) - b_{c1} + m_{c1}(pn - p0) + e_{an(pn,q1),c1(pn,q1)} \\
y_{an(pn,qn)} - y_{cn(pn,qn)} &= b_{an} + m_{an}(qn - q0) - b_{cn} + m_{cn}(pn - p0) + e_{an(pn,qn),cn(pn,qn)}
\end{aligned}
$$

Equation 8

This system can be formed in the matrix of the observation model in term of least-squares adjustment with fixed constraints (Koch, 1999 and Surpas, 2003) as follows:

$$Y = AX + e$$

Equation 9

where Y represents the vector of observed differences, A is the design or coefficient matrix relating the observation to the unknown, X, and e is the residual. The constraints matrix is formed based on the fixed-constraint condition as:

$$K_0 = KX$$

Equation 10

where K_0 is the vector of fixed constraint values, K is the matrix that relates the unknown parameter, X, to the designed matrix (A). The unknown parameter, $\hat{X}$, is determined by the least-squares adjustment as:

$$\hat{X} = (N + K^TK)^{-1}C + (N + K^TK)^{-1}K^T[K(N + K^TK)^{-1}K^T][K_0 - (N + K^TK)^{-1}C]$$

Equation 11

where $N=A^TPA$, $C=A^TPY$ and P is a weight matrix. For simplicity, we define P as an identity matrix. The air-controlled or constraint points were selected from the set of cross-over points.

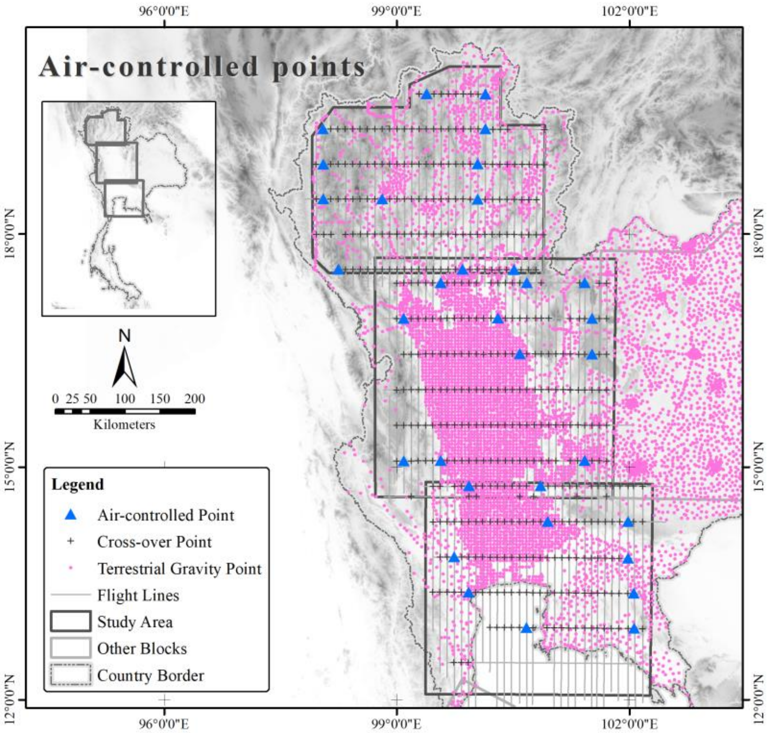

Figure 5: The air-controlled points (blue triangle dots) and terrestrial gravity points (magenta dots)

The selection followed two optimal conditions: (1) the FAA differences at the crossing points were within the limit of ±2mGals, and (2) the FAA data of along-tracks and cross-tracks did not differ more than ±2mGals from the computed FAA using the terrestrial gravity data points in Chao Phraya basin. The computed FAA were obtained from the gravity values on the ground by means of an upward continuation using a least-squares collocation (the collocation method is not be addressed in this study; see Heiskanen and Moritz (1967) for more details). There were a total of 33 air-controlled points, and the optimal adjustment resulted from selecting control points that covered as much of the block edges as possible. Therefore, most of them were distributed on the edges of each block, as shown in Figure 5.

5. Airborne Gravity Geoid Determination

The geoid determination in this study was based on Molodensky's approach, which derives geoid undulation from a height anomaly, ζ, by using Bouguer anomalies, Δg_B, as in the following equation (Heiskanen and Morits, 1967):

$$N \approx \zeta + \frac{\Delta g_B}{\gamma_0} H$$

Equation 12

where H is orthometric height and γ_0 is a normal gravity. The calculation of height anomalies from airborne FAA was started by applying a terrain correction using a residual terrain (RTM) model with a one arc-minute Thailand digital elevation model. This was then reduced to an MSL using a least-square collocation (LSC) approach.In this principle, a height anomaly was computed by a Fast Fourier Transform (FFT) which required a mean gravity anomaly, $\Delta\bar{g}$., covering the whole surface. The $\Delta\bar{g}$ computation is as follows:

$$\Delta\bar{g} = C_{\Delta\bar{g}\Delta g}(C_{\Delta g\Delta g} + D_{\Delta g\Delta g})^{-1}\Delta g$$

Equation 13

where $C_{\Delta\bar{g}\Delta g}$ and $C_{\Delta g\Delta g}$ are covariance matrices between predicted and observed values respectively, and Δg is the observed values. The $C_{\Delta g\Delta g}(.)$ elements of $C_{\Delta g\Delta g}$ is a planar covariance model between observation values under isotropic and stationary assumptions and $D_{\Delta g\Delta g}$ denotes the covariance matrix between noises under white noise assumption (Forsberg, 1987). The $C_{\Delta g\Delta g}(.)$ equation is:

$$C_{\Delta g\Delta g}(\Delta g^{h_1}, \Delta g^{h_2}) = -C_0 \sum_i \alpha_i log(D_i + \sqrt{s^2 + (D_i + h_1 + h_2)^2}) \text{ with } D_i = D - iT$$

Equation 14

where C_0 is a variance component, D is Bjerhammar sphere depth, T is a long-wavelength attenuation, s is the distance between observation points, and α_i is the coefficient at i that needs to be determined through trial and error (D, and T) a priori to use Equation (3) (Forsberg and Tscherning, 2008.)

6. Cross-Over Adjustment and Geoid Determination Results

The difference between FAA values at intersections of an along-track and cross-track theoretically yields a variance of zero. However, zero cross-over differences rarely appear in practice. Due to severe weather conditions during airborne surveys, the differences actually ranged between -24 and +30 mGals. We considered differences exceeding the limits of ±15mGals as outliers, and they were not used for the cross-over adjustment computations. Large cross-over differences occurred in mountainous areas, with terrain masses that could significantly affect observed gravities along survey lines. The drift of TAGS-6 was three mGals per month or less. Such a dynamic error was negligible as each survey session lasted for under 4 hours. The distribution of cross-over differences showed an approximately normal distribution, implying that a significant cause of these dissimilarities was random noise (this distribution agreed with Moritz, 1980) (Figure 6a.)

In this study, we only considered systematic errors along survey lines in the airborne gravimetric data. Such constant errors were represented by the simple linear trend of each survey line, according to Equation (4) to Equation (7). The cross-over least-squares adjustment followed Equation (8) to Equation (10). In Figure 5, controlled or fixed points served as reference points for the constraint condition in Equation (11). These control points were selected from the cross-over points, which the FAA differences between along and cross-tracks should not exceed the limits of ±2mGals. Cross-over adjustments reduced FAA differences at the cross-over points by considering not only the slope and intercept of the linear equation that fitted each survey line but also the adjustment of selected control points at which FAA was less than 2 mGals of the intersection differences. The results showed that the root mean square (RMS) of the differences was reduced from 3.916 to 2.596 mGals, as demonstrated in Table 2. The average standard error of the airborne gravimetric data in this study was about 2.598/√2 ≈

1.836 mGals. Figure 6b shows how the adjustment reduced the differences. Figure 7 presents a histogram of the FAA differences at cross-over points before and after the adjustment. Clearly, the adjustment reduced the cross-over differences. The cross-over adjusted and non-adjusted FAA, after reduced the terrain effect by applying the residual terrain model approach, then downward continued to MSL using LSC in Equation (14). The relationship between airborne gravity variances and distances is shown in Figure 7. The observed gravities are correlated within 35km for a variance of 67 $mGal^2$ with D = 2km and T=127km. The accuracy of both cross-over adjusted and non-adjusted airborne geoid models was evaluated using a geoidal height of 184 GNSS/Leveling co-point stations. As shown in Table 3, the comparative results showed a slight improvement of the root mean square of the adjusted geoid model from 0.10m to 0.89m.

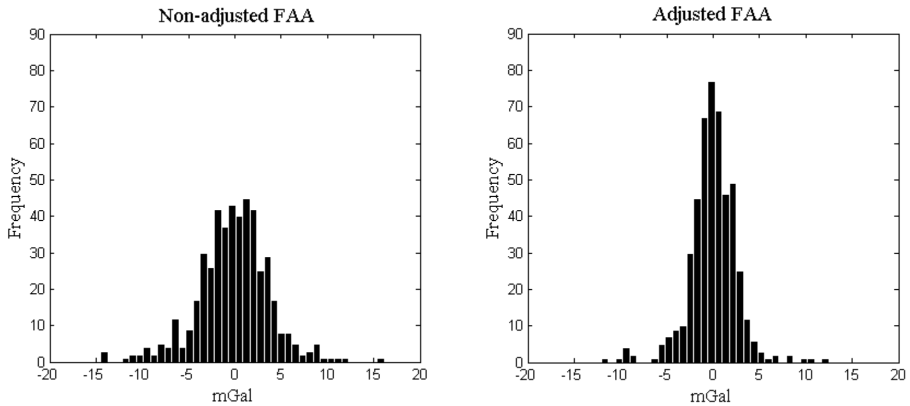

(A) (B)

Figure 6: Histogram of FAA differences at the intersection before (A) and after (B) least-square adjustment with fixed constraints

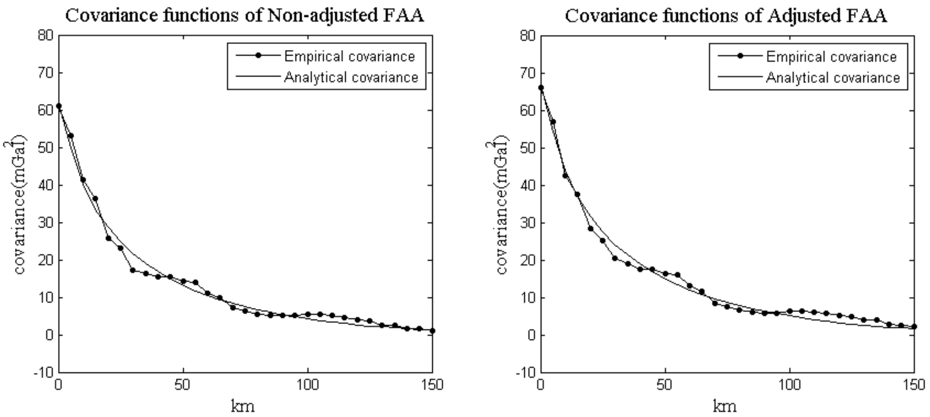

(A) (B)

Figure 7: Empirical (dot line) and analytical-planar (thin line) covariance models of non-adjusted (A) and adjusted (B) free air anomalies

Table 2: Statistics of FAA differences at cross-over points (mGals)

Case	Min	Max	Mean	S.D.	RMS
Non-Adjusted	-14.455	16.125	-0.148	3.917	3.916
Adjusted	-12.077	12.355	-0.067	2.618	2.616

Table 3: Comparative results of adjusted and non-adjusted airborne-geoid models to the GNSS/Leveling control stations

Geoid	Min (m.)	Max (m.)	Mean (m.)	S.D. (m.)	RMS (m.)
Non-adjusted	-0.256	0.231	-0.020	0.089	0.102
Adjusted	-0.255	0.231	-0.019	0.085	0.089

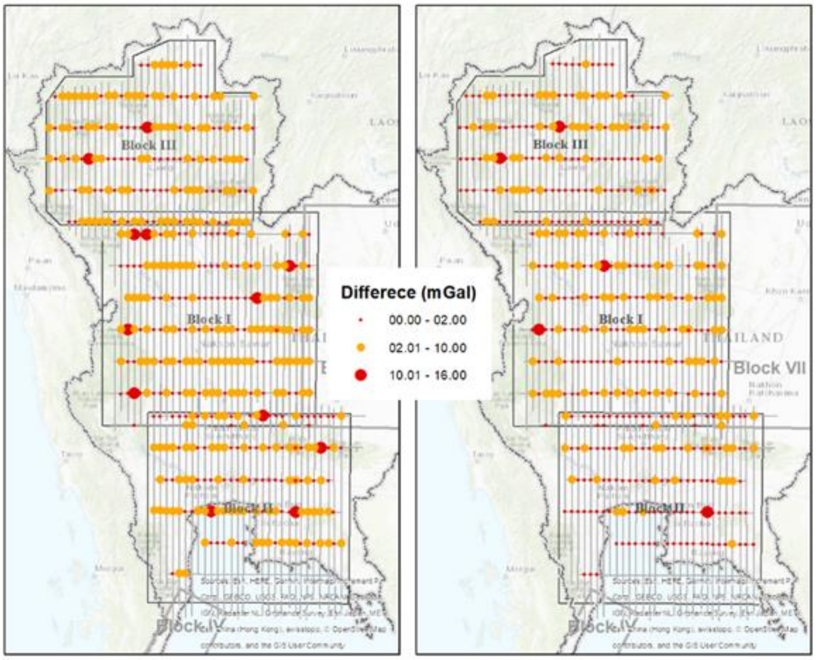

(A) (B)

Figure 8: The cross-over differences before (A) and after (B) the cross-over least-squares adjustments of survey lines

7. Conclusions

Airborne gravimetry in the Chao Phraya basin was conducted in May 2016 at a 4,000m flight altitude with 10km along-track spacing and 50km cross-track spacing. The airborne gravimetric data was contaminated with strong noises due to weather-related air turbulence. The preliminary inspection and editing and cross-over adjustments were considered for data preparation before a precise geoid determination was made. After the filtered FAA was compared with EGM2008 data from the same location and altitude, any unusual data ranges were edited and modified. Other related measurement information at the same time and location, including beam movement and the number of high vertical accelerations, were considered. We found three lines with contaminated noises that exceeded a 50% difference, and re-flights were done in lines 106, 123 and 129 of Block 1. The linear trend adjustment was constrained using 33 selective cross-over points. Most of these points were distributed on block edges. An LSA with constraints reduced the differences in FAA values from the cross-over points presented in Figure 8. The results showed that the root mean square (RMS) of the difference at the cross-over points was reduced from 3.916 to 2.596 mGals. This study took advantage of terrestrial gravimetry for reference data. The accuracy of the airborne gravimetric data in this study was about 1.836 mGals, corresponding to an improvement in the accuracy of the airborne geoid models, going from 0.100m to 0.890m. The proposed approach using cross-over adjustments with constants showed an improvement in the accuracy of geoid models. As the airborne gravity data sets improve, the adjustment results will be correspondingly better. However, the accuracy of the geoid is sensitive to the number and locations of air-controlled points for large areas of geoid determination in Thailand. Further works of optimal cross-over locations have to be envisioned and efforts should be made to improve the quality of airborne gravimetric data.

Acknowledgment

The authors would like to express our great appreciation to Maj. Gen. Chaiwat Promtong for his support. We also would like to thank all staff in the Aerial Survey and Geodesy & Geophysics Divisions, Royal Thai Survey Department, for their assistance and relevant data sets. Our special thanks are extended to Prof. Dr. Rene Forsberg for his constructive suggestions.

References

Albert, B. and Klees, R., 2004, A Comparison of A Method for the Inversion of Airborne Gravity. *Journal of Geodesy*, Vol. 78, 55-65.

Bayoud, F. A. and Sideris, M. G., 2002, Geoid Determination from Airborne Gravity Data Using

Different Filtering Frequencies and DTM Resolutions. *Vistas for Geodesy in the New Millennium*, 217–222. doi:10.1007/978-3-662-04709-5_36.

Damiani, T. M. and Youngman, M. A., 2015, *GRAV-D General Airborne Gravity Data User Manual*. National Geodetic Survey, US. Available online as of 4 August 2015: http://www.ngs.noaa.gov/GRAV-D/data/NGS-_GRAV-D_General_Airborne_Gravity_Data_-User_Manual_v2.0.pdf

Dumrongchai, P., Wichienchareon, C. and Promtong, C., 2012, Local Geoid Modeling for Thailand. *Int. J. of Geoinformatics*, Vol. 8(4), 15-226.

Dumrongchai, P., Srimanee, C. Duangdee, N. and Promtong, C., 2017, Preliminary Results of Airborne Gravimetry for geoid Determination in Chao Phraya Basin. *Journal of RESGAT*, Vol. 18(4), Special Issue, 269-280.

Dumrongchai, P. and Duangdee, N., in press. Evaluation of TGM2017 for Height System Using GNSS/Leveling Data in Thailand. *International Transaction Journal of Engineering, Management, & Applied Sciences & Technologies*.

Forsberg, R., 1987, A. new covariance model for inertial gravimetry and gradiometry, *J. Geophys*. Res., vol. 92, no. B2, 1305-1310.

Forsberg, R., Olesen, A., Bastos, L., Gidskehaug, A., Meyer, U. and Timmen, L., 2000, Airborne Geoid Determination. *Earth Planets Space*, Vol. 52, 863-866.

Forsberg, R., 2005, Towards a CM-Geoid for Malaysia. Sound/Visual Production (Digital), Retrieved from http://www.jupem.gov.my/JUP-EM/RTKnet/Toward_a_cmgeoid.pdf

Forsberg, R., Olesen, A., Bastos, I. and Einarsson, 2015, Airborne Gravimetry for Geoid with Lacoste Romberg and Chekan Gravimeters. *Gyroscopy and Navigation*, Vol. 6(4), 19-29.

Forsberg, R. and Tscherning, C., 2008, *An Overview Manual for the GRAVSOFT Geodetic Gravity Field Modelling Programs*, National Space Institute (DUT-Space) and Niels Bohr Institute, U. of Copenhagen, Denmark.

Heiskanen, W. and Moritz, H., 1967, *Physical Geodesy*. (San Francisco: WH Freeman).

Hwang, C., Hsiao, Y., Shih, H., Yang, M., Chen, K. and Forsberg, R., 2007, Geodetic and Geophysical Results from a Taiwan Airborne Gravity Survey: Data Reduction and Accuracy Assessment. *Journal of Geophysical Research*, Vol. 112, B04407, doi:10.1029/2005JB004220.

Koch, K. R., 1999, *Parameter Estimation and Hypothesis Testing in Linear Models*, 2nd edition, (Berlin: Springer).

Li, Y., 2000, Airborne Gravimetry for Geoid Determination. PhD Thesis, University of Calgary, Department of Geomatics Engineering, Report No. 20141.

Micro-g LaCoste, 2015a, TAGS-6/MGS-6 PiperPro Processing Software Manual. Colorado. Micro-g LaCoste.

Micro-g LaCoste, 2015b, *TAGS-6 Turnkey Airborne Gravity System AeroGrav Data Processing Manual*. Colorado. Micro-g LaCoste.

Moritz, H., 1980, *Advanced Physical Geodesy*. (Karlsruhe: Herbert Wichmann).

Olesen, A. V., 2003, *Improved Airborne Scalar Gravimetry for Regional Gravity Field Mapping and Geoid Determination*. Technical Report, National Survey and Cadastre, Denmark (KMS).

Pavlis, N. K., Holmes, S. A., Kenyon, S. C. and Factor, J. K., 2012, The Development and Evaluation of the Earth Gravitational Model 2008 (EGM2008), *Journal Geophysical Research*, Vol. 117, B04406, doi:10.1029/2011JB008916.

Srimanee, C., Dumrongchai, P. and Doungdee, N., 2018, The Improvement of Airborne Gravity Data in Chao Phraya Basin Using Cross-Over Adjustment. *Proceedings of the 33rd International Technical Conference on Circuits/Systems, Computers and Communications*. July 4-7, 2018, Bangkok, Thailand.

Surpas, J. G., 2003, *Local and Regional Geoid Determination from Vector Airborne gravimetry*. Dept. of Civil and Environmental Engineering and Geodetic Science, (Ohio: The Ohio State University).